



Nanohydroxyapatite Loaded-Acrylated Polyurethane Nanofibrous Scaffolds for Controlled Release of Paclitaxel Anticancer Drug

Mirmehdi Seyyedi^{1*}, Amir Molajou²

¹ University of Wyoming, United States

² Iran university of science and technology, Iran

Abstract

Nanofibers prepared by electrospinning process with high specific surface area, high porosity and interconnected pores are good candidates for drug delivery systems. In the present study, the acrylated polyurethane/nanohydroxyapatite (APU/n-HAp) nanocomposite nanofibers were fabricated via electrospinning method for controlled release of paclitaxel (PTX). Poly(ϵ -caprolactone) diol (PCL), aliphatic 1,6-hexamethylene diisocyanate (HDI) and hydroxyethyl methyl acrylate (HEMA) were used for synthesis of APU. The APU/n-HAp nanocomposite fibers were characterized using X-ray diffraction (XRD), scanning electron microscopy (SEM), swelling and mechanical tests. The increase in mechanical properties was achieved by incorporating of n-HAp nanoparticles up to 5% into the APU. The swelling behavior results indicated that the hydrophilicity of APU/n-HAp nanocomposite fibers and water uptake were increased by increasing n-HAp content. The initial burst release and following the sustained release of paclitaxel from nanofibers was obtained during 120 h. The obtained results suggested that the APU/n-HAp 5% nanocomposite nanofiber could be considered for delivery of anticancer drugs.

Keywords

Acrylated Polyurethane, Hydroxyapatite Nanoparticles, Nanocomposite, Nanofiber, Anticancer Drug

1. Introduction

Nanofibers prepared by electrospinning process have been developed and considered as good candidates for loading of various drugs (Khodadadi et al., 2020; Rasouli et al., 2020; Dizaji et al., 2020; Farboudi et al., 2020a; Abasian et al., 2019; Bahmani et al., 2020; Qavamnia et al., 2020). Among nanofibers used for drug delivery systems (DDSs), the hydrophobic polymers could be used for sustained delivery of anticancer drugs (Farboudi et al., 2020b; Radmansouri et al., 2018; Jouybari et al.,

* Corresponding Author: University of Wyoming, United States

E-Mail Address: mseyyedi@uwyo.edu

2019). However, the sustained release of drug and high drug release percentage after a long time should be simultaneously occurred for optimized carrier. The low drug release percentage is the most challenge of nanofibers prepared by hydrophobic polymers. To overcome this problem, the hydrophilic polymers were blended with hydrophobic polymers or hydrophilic fillers such as metal oxides and bioactive materials were loaded into the hydrophobic nanofibers (Irani et al., 2017; Aboutalebi Anaraki et al., 2015; Demir et al., 2018; Eskitoros-Togay et al., 2019; Ghafoor et al., 2018).

In recent years, polyurethanes (PUs) have been widely used in various biomedical applications such as cardiovascular repair, cartilage implant, ligament regeneration, bone replacement and drug delivery (Yao et al., 2008; Guelcher, 2008; Hofmann et al., 2008). The PUs are formed from three basic building blocks including the polyol, an isocyanate and a chain extender (Krol, 2007). The PUs chains consist of urethane based hard segment and polyether or polyester based soft segment (Krol, 2007). The various ratio of hard and soft segments in the structure of PUs caused to have unique properties such as excellent physicochemical and mechanical resistance as well as good biocompatibility (Tawa & Ito, 2006). These properties led to incorporate the PUs in fabrication of different biomedical devices (Guelcher et al., 2005; Pereira et al., 2010). However, the long term molecular stability is one of important limitation of PUs in design of biomedical devices. In order to overcome the limitation, the PUs can be modified by an acrylic functionality such as 2-hydroxy-ethylacrylate (HEA) or 2-hydroxyethyl methacrylate (HEMA) to produce the acrylated polyurethanes (APUs) (Alishiri et al., 2014; Ouyang et al., 2015; Bao & Shi, 2010; He et al., 2010; Wang et al., 2008). The hard segment of APUs is formed by isocyanate and HEA or HEMA and the soft segment consist of polyether or polyester polyol. The presence of HEA or HEMA in the structure of APUs reduce the viscosity of APUs prepolymers and provide to the APUs better light stability, better flexibility and higher degradation rate than PUs (Alishiri et al., 2014; Ouyang et al., 2015; Bao & Shi, 2010; He et al., 2010; Wang et al., 2008).

Hydroxyapatite (HAp), with the general formula $\text{Ca}_{10}(\text{OH})_2(\text{PO}_4)_6$, due to the similar chemical composition and structure to the mineral phase of human bone, have been widely used as a bone substitute and replacement in biomedical applications (Shackelford, 1999; Nunes et al., 1997). Nano-sized materials due to their exclusive properties, such as large external surface area and activities have been widely used in biomedical applications (Boissard et al., 2009). Nano-hydroxyapatite (n-HAp) due to their greater surface area have shown better protein adsorption and bone cell adhesion compared with micro-sized HAp (Boissard et al., 2009; Webster et al., 1999). However, the use of n-HAp due to the intrinsic hardness, fragility, and lack of flexibility is limited (Chen & Wang, 2000). In order to overcome the drawbacks of n-HAp, the nanoparticles have been loaded/blended with various types of polymeric nanofibers to enhance the mechanical and bioactive properties (Suslu et al., 2014). In previous studies, the composite nanofibers containing n-HAp were applied for biomedical applications such as drug delivery and bone regeneration (Chen & Chang, 2011; Rajzer, 2014; Tsai et al., 2018; Zheng et al., 2013a; Zheng et al., 2013b).

In the present study, a novel nanofibers based on APU/n-HAp was synthesized and characterized using XRD, SEM and tensile analysis. The potential of APU/n-HAp nanocomposite nanofibers was investigated for sustained delivery of paclitaxel.

2. Experimental

2.1. Materials

Poly (caprolactone) ($M_n=2000 \text{ g mol}^{-1}$, PCL), 2-Hydroxyethyl methacrylate (HEMA) and 2, 2-

azobisisobutyronitrile (AIBN) were purchased from Sigma-Aldrich (Germany). 1, 6-Hexamethylene diisocyanate (HDI), ethylene glycol dimethacrylate (EGDMA) were provided from Merck (Germany). n-HAp of 20–30 nm crystallite size was obtained from Sigma-Aldrich (USA).

2.2. Synthesis of Acrylated Polyurethane (APU)

Isocyanate terminated prepolymers were synthesized by PCL and HDI according to a standard two-step polymerization as described previously (Guelcher et al., 2007). Briefly, PCL and HDI (1:2 by mole) were poured into a 250 mL reactor flask equipped with heating mantle, reflux condenser, mechanical stirrer, dropping funnel and nitrogen gas inlet system. The mixture was heated to 60 °C and maintained for 2 h with stirring; then, the temperature increased to 85°C and the reaction was carried out for over 1 h to the NCO content reached the theoretical value, as determined by dibutylamine titration (Guelcher et al., 2007). Thus, after the theoretical NCO value was achieved at the end of the above procedure, the reaction flask was cooled down to 40°C. Then, HEMA was added drop wise into the flask and the reaction was continued for over 30 min with stirring. The mole ratio of PCL/HDI/HEMA during synthesis was kept on 1:2:2 in this step. Then the temperature was heated up to 80 °C slowly. The reaction was continued at temperature of 80 °C until the NCO peak at 2270 cm^{-1} was disappeared in the Fourier transform infrared (FTIR) spectrum.

2.3. Synthesis of APU/n-HAp Nanocomposite

The HAp nanoparticles were dispersed in acetone by stirring it for 2 h. Then n-HAp solutions were added to the previously prepared APU solutions. After that, the HEMA and EGDMA with weight ratio of 70/30 were added to the mixtures and the reaction was continued for further 2 h with stirring. Then, AIBN (1 wt. %) was added to the mixtures for initiating crosslink reaction through the vinyl end groups. The mixtures were poured into the glass mold and were cured under vacuum for 10 min at room temperature. Finally, the prepared molds were placed at 95°C for 8 h. The APU/n-HAp nanocomposites containing 2, 5 and 7 wt.% of n-HAp with respect to the total solution concentration were prepared in the same way.

2.4. Fabrication of APU/n-HAp Nanocomposite Fibers

Aqueous 10 wt.% APU solutions were prepared by dissolving of APU in DMF. The prepared solutions were loaded into the 5 mL plastic syringe equipped with a syringe needle. This was placed to a KD programmable syringe pump to control the solution feeding rate. High voltage is applied between a needle and a cylindrical collector and nanofibers were produced on the collector surface. A voltage of 20 kV, tip collector distance of 14 cm, feeding rate of 0.5 mL h^{-1} , and speed collector of 500 rpm was applied to produce the nanofibers on collector. Then, the nanofibers were dried for 24 h at 60 °C.

To load paclitaxel molecules into the nanofibers 50 and 100 μg paclitaxel were added into the 5 mL electrospinning solution before electrospinning process.

2.5. Characterization Tests

The structure and crystallinity of APU/n-HAp nanocomposite fibers were determined using STADI P X-ray diffractometer (XRD, STOE Co., Germany) with Cu/K α ($\lambda = 1.542 \text{ \AA}$) radiation over Bragg angles ranging from 10 to 60° at a scanning rate of 0.2°/min. The morphology of synthesized APU/n-HAp nanocomposite fibers was characterized using a scanning electron microscope (TESCAN Co, Czech Republic) after gold coating. The tensile properties were measured by HIWA 2126 universal

testing machine (HIWA Engineering Co., Iran) at room temperature, while the crosshead speed was 2 mm min⁻¹ and the dumbbell-shaped nanocomposites were prepared according to ASTM-D638. The swelling property of the nanocomposites (10 × 10 × 1 mm) was evaluated by weight change of the sample in the nanocomposites before and after soaking in deionized water for 1, 2 and 3 days at 37 °C. All experiments were repeated at three times. The swelling percentage was calculated by:

$$\text{Swelling}(\%) = \frac{W_w - W_d}{W_d} \times 100 \quad (1)$$

Where W_w and W_d are the masses of the swollen and dried samples, respectively. The contact angle (CA) of the prepared nanocomposites was measured by data physics OCA15 plus (Instruments GmbH, Germany) at room temperature.

2.6. Drug Loading Efficiency and Release Studies

To investigate the drug loading efficiency (DLE), the prepared nanofibers were first dissolved into the DMF solvent. The absorbance of paclitaxel was measured using HPLC analysis at 256 nm. DLE (%) is evaluated as follows:

$$\text{DLE}(\%) = \frac{\text{Final content of drugs in fibers}}{\text{Initial content of drugs doped -fibers}} \times 100 \quad (\text{Eq. 1})$$

To investigate the paclitaxel release manner from nanofibers, various paclitaxel content (50 and 100 µg), the drug loaded-nanofibers were incubated in 50 mL of PBS solution under stirring at 37 °C under pH of 7.4 for 30 days. At predetermined time intervals, 2 mL of incubation solution was collected from the solution medium to measure the paclitaxel content using HPLC analysis at 256 nm. While, 2 mL of fresh PBS was simultaneously added into the dissolution medium. The paclitaxel release percentage was determined according to its concentration at certain time and initial drug content in nanofibers. The release experiments were carried out three times and the average values were reported.

3. Results and Discussion

3.1 XRD Analysis

The XRD patterns of APU and APU/n-HAp nanocomposite fibers are shown in Fig. 1. As shown, the broad weak peak around $2\theta=19^\circ$ were present in all samples which correspond to APU polymer. The sharp diffraction peak at $2\theta=31.86^\circ$ indicating the formation of n-HAp crystal on the polymer matrix. Moreover, the XRD patterns of the APU/n-HAp nanocomposite fibers showed the sharp peaks with higher crystallinity compared with pure APU. The APU and APU/n-HAp 5% nanocomposite fibers had crystallinity of 36% and 80%, respectively.

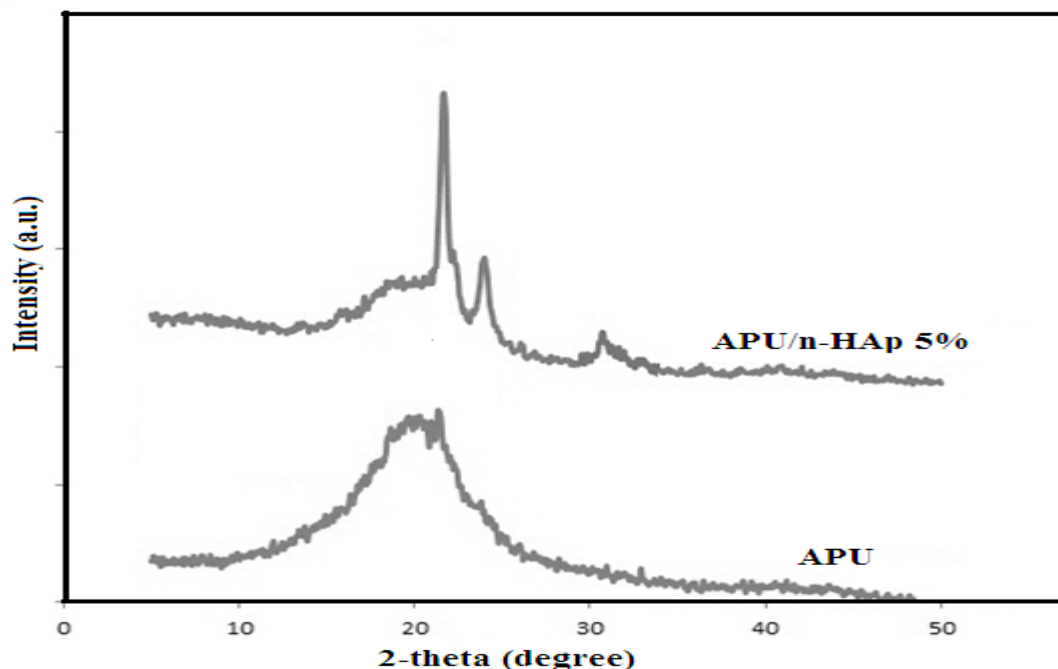


Fig.1. XRD patterns of APU and APU/n-HAp 5% nanocomposite fibers

3.2. Mechanical Properties

The tensile strength–strain curves for APU and APU/n-HAp 5% nanocomposite fibers are shown in Fig. 2 and the mechanical properties are summarized in Table 1. Based on results, the tensile moduli and tensile strength improved by incorporation of n-HAp into the APU matrix. Whereas, the higher elongation at break for pure APU was observed. The tensile modulus and tensile strength varied from 57.5 and 12.2 MPa for the pure APU up to 78.9 and 14.7 MPa for the APU/n-HAp 5%, respectively. This behavior could be attributed to the higher crosslink density, additional hydrogen bonding between n-HAp and APU, higher degree of phase separation and decline the mobility of polymer chains by incorporation of n-HAp nanoparticles into the APU matrix (Wang et al., 2010).

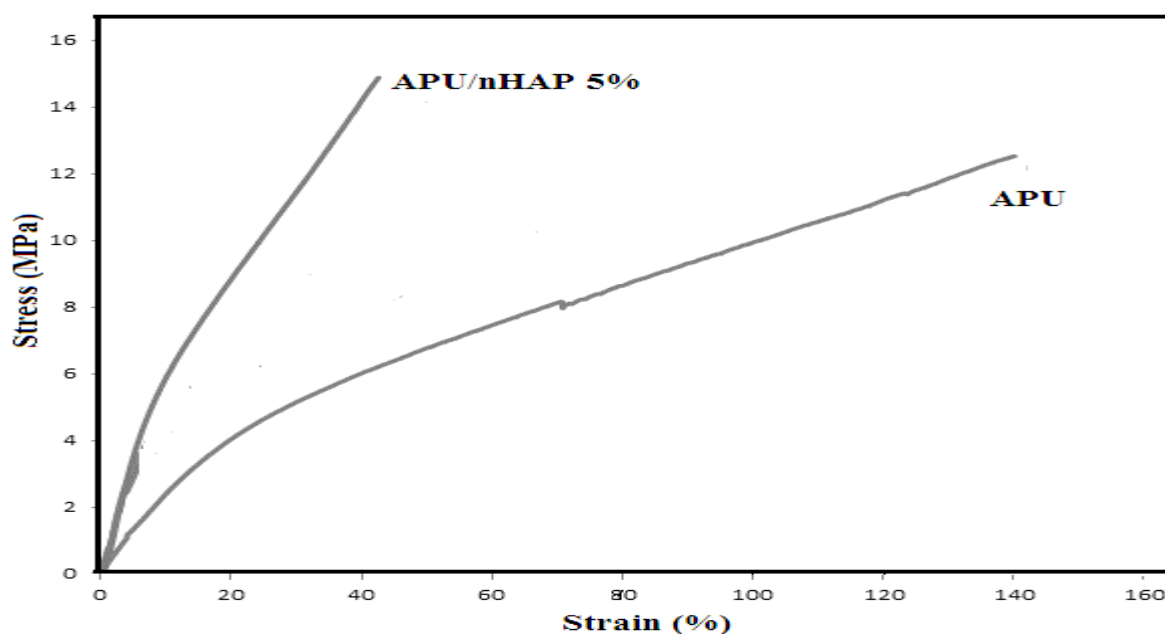


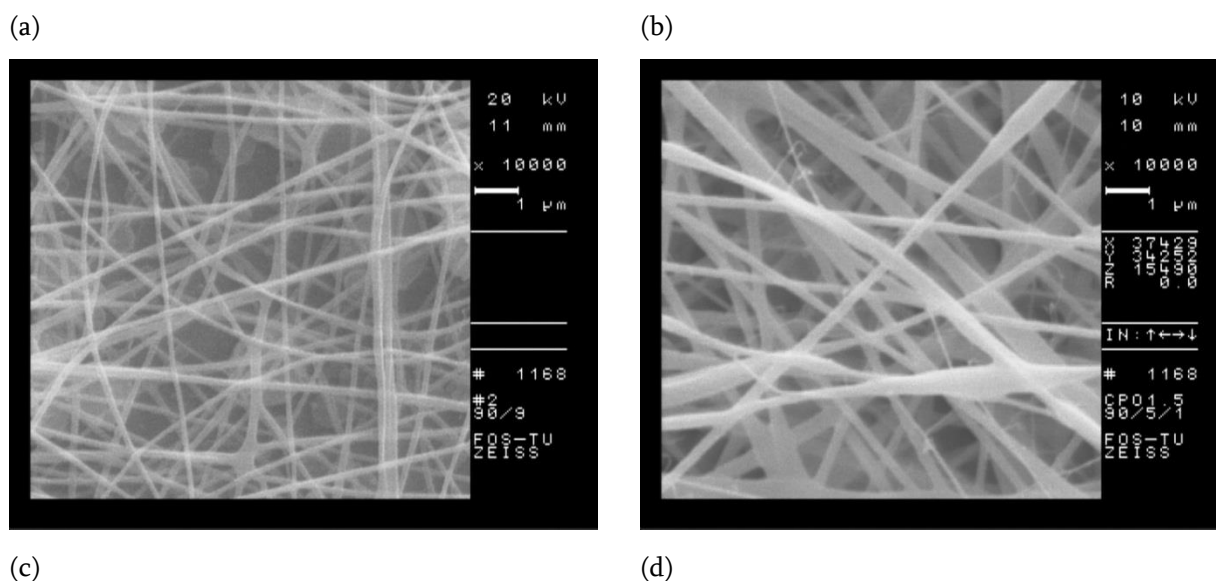
Fig. 2. Strength–strain curves for APU and APU/n-HAp 5% nanocomposite fibers**Table 1.** Tensile properties of pure APU and APU/n-HAp nanocomposite fibers

Sample	Yong's Modulus (MPa)	Tensile Strength (MPa)	Elongation at Break (%)
APU	57.5±2	12.2±0.3	1060±30
APU/n-HAp 1%	64.3±2	12.9±0.2	670±20
APU/n-HAp 2%	73.4±3	13.7±0.4	410±25
APU/n-HAp 5%	78.9±3	14.7±0.3	330±30

3.3. SEM Images

The SEM images of APU and APU/ n-HAp nanocomposite containing 2%, 5% and 7% n-HAp are illustrated in Fig. 3. As shown, the uniform nanofibers ranging from 100-250 nm with an average diameter of 180 nm was produced for APU nanofibers under applied voltage of 20 kV, tip collector distance of 14 cm, feeding rate of 0.5 mL h⁻¹, and speed collector of 500 rpm. The well dispersion of n-HAp up to 5 wt.% indicated the good interfacial bonding between the polymer and n-HAp nanoparticles for synthesized APU/n-HAp nanocomposite fibers. The average diameter of APU/n-HAp nanocomposite fibers containing 2% and 5% n-HAp were increased to 260 nm and 290 nm, respectively due to physical loading of n-HAp into the nanofibers. By increasing the n-HAp content to 7%, the more nanoparticles were aggregated on the nanocomposite fibers surface.

SEM images of APU/ n-HAp 5% nanocomposite fibers and PTX loaded- APU/ n-HAp nanocomposite fibers are illustrated in Fig. 4. The comparison of the surface morphologies of APU/ n-HAp 5% nanocomposite fibers and PTX loaded- APU/ n-HAp nanocomposite fibers demonstrated the well loading of drug molecules on the nanofibers surface without aggregation. Furthermore, the average fiber diameter was increased from 290 nm to 360 nm by loading of PTX (100 µg) into the nanofibers.



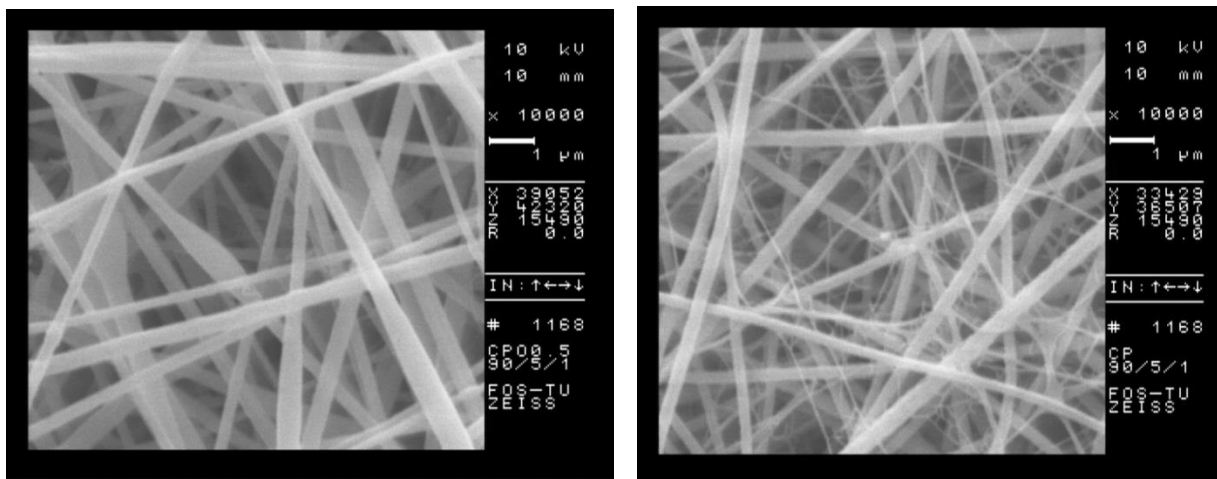


Fig. 3. SEM images of (a) APU and APU/ n-HAp nanocomposite fibers containing (b) 2%, (c) 5% and (d) 7% n-HAp

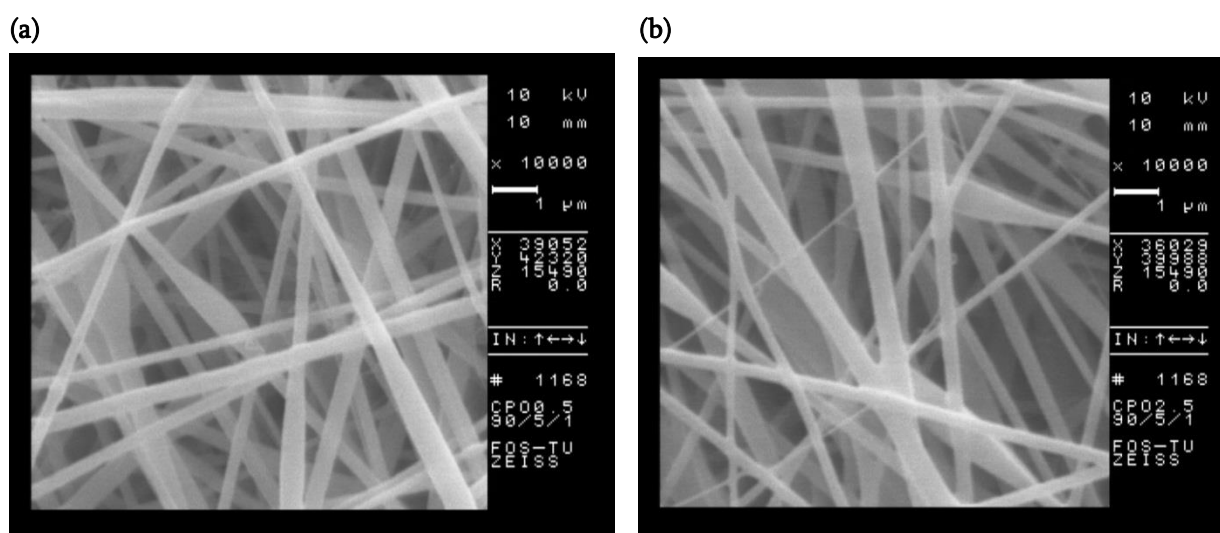


Fig. 4. SEM images of (a) APU/ n-HAp 5% and (b) PTX loaded- APU/ n-HAp nanocomposite fibers

3.4. Swelling

The swelling ratios of the nanofibrous scaffolds measured by water uptake (%) and water contact angle ($^{\circ}$) are listed in [Table 2](#). The hydrophilic nature of HAp nanoparticles resulted in increasing the water uptake and contact angle of APU matrix. The water uptake of pure APU fibers due to the hydrophobic nature of APU was low. By incorporation of n-HAp into the APU matrix and increase in n-HAp content, the water uptake percentage due to increase in the number of hydrophilic groups such as O-H and PO_4^{3-} in the APU network, was increased. The water contact angle measurement results indicated that the pure APU nanofibers had a contact angle of 66° . The contact angle of APU/n-HAp nanocomposite fibers due to the improvement of hydrophilic properties of fibers was decreased from 66 to 52° by increasing n-HAp content to 5%. At higher n-HAp content than 5%, the aggregation of nanoparticles and blockage of the APU matrix pores resulted in increasing water contact angle to 58° .

Table 2. Water uptake and contact angle of synthesized fibers

Fibers	Water Uptake (%)			Water Contact Angle (°)
	24 h	48h	72 h	
APU	4.65±0.1	4.98±0.1	5.31±0.05	66.0±0.5
APU/n-HAp 1%	6.32±0.1	7.92±0.15	9.08±0.05	60.5±0.5
APU/n-HAp 2%	7.84±0.1	9.03±0.2	11.10±0.1	56.5±0.5
APU/n-HAp 5%	9.37±0.2	10.50±0.2	12.90±0.1	52.0±0.5
APU/n-HAp 7%	12.12±0.2	13.90±0.2	16.80±0.1	58.0±0.5

3.5. Drug Loading Efficiency, Drug Release from Nanofibers

The drug loading efficiency of nanofibers is presented in Table 3. As shown, the PTX loading efficiency was found to be higher than 90% for all synthesized nanofibers. The gradual lower drug loading efficiency for nanofibers containing n-HAp could be attributed to the bonding of PTX molecules into the n-HAp particles. The obtained results demonstrated the high encapsulation of PTX molecules into the nanofibers.

Table 3. Drug loading efficiency of synthesized UiO-66-NH₂/DOX/PNVCL NMOFs (n=5)

N-HAP Concentration (%)	PTX Concentration (µg ^m -1)	Drug Loading Efficiency (%)
0	50	98.5±1.1
2	50	95.9±1.6
5	50	94.6±1.5
7	50	92.2±1.4
2	100	93.9±1.3
5	100	91.9±1.6
7	100	90.6±1.5

The PTX release profiles from APU/PTX and APU/n-HAp 5%/PTX are illustrated in Fig. 5.

As shown, the burst release of 12.2, 15.3, 18.9 and 23.1% PTX from APU/PTX 50 µg, APU/PTX 100 µg, APU/n-HAp 5%/PTX 50 µg and APU/n-HAp 5%/PTX 100 µg nanofibers were observed during 12 h. This behavior could be attributed to presence of PTX molecules on the surface/pores near the surface of nanofibers. After that the continuous release percentages were found to be 80.2%, 82.3%, 84.9% and 87.6% after 120 h incubation time. By loading n-HAp into the nanofibers, the release percentage was gradually increased. Although, the hydrophilic nature of n-HAp nanoparticles could be resulted in the faster release of drug molecules, the filling of some pores of nanofiber with n-HAp nanoparticles prevented the diffusion of PTX molecules into the pores and its release from nanofibers which neutralized the effect of hydrophilicity on the release rate of PTX and resulted in gradually increase in drug release percentage. The lower distance of PTX molecules in APU and APU/n-HAp nanofibrous matrix through the loading higher content of PTX resulted in faster release of 100 µg PTX loaded-nanofibers in comparison to 50 µg PTX loaded-nanofibers.

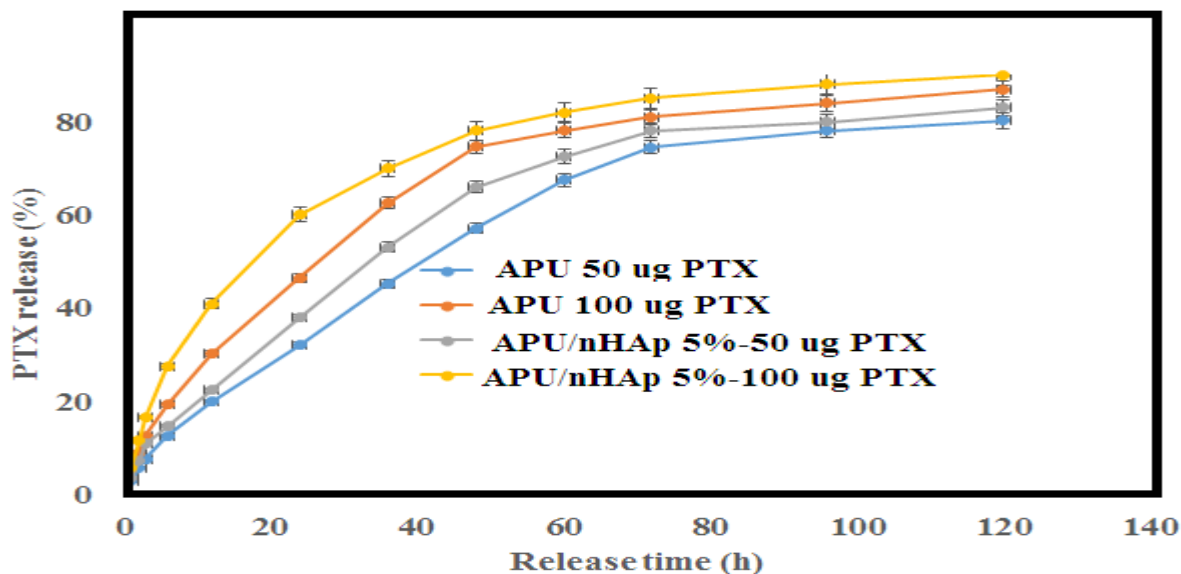


Fig. 5. PTX release from synthesized nanofibers containing PTX

4. Conclusion

In this work, APU/n-HAp nanocomposite nanofibers were successfully fabricated by electrospinning process for controlled release of PTX. The XRD patterns of samples demonstrated the formation of n-HAp crystals on the nanofibers matrix. The tensile modulus and tensile strength were increased from 57.5 and 12.2 MPa to 78.9 and 14.7 MPa by loading of n-HAp 5% into the APU fibers. The average fiber diameters of APU and APU/n-HAp 5% were found to be 180 nm and 290 nm, respectively. Loading PTX molecules into the nanofibers resulted in increasing fiber diameter to 360 nm. Increase in the HAp content in nanofibers led to increase water uptake and decrease the contact angle of nanofibers. The drug loading efficiency was found to be higher than 90% for nanofibrous samples containing PTX. The continuous release of PTX (>80%) was obtained from nanofibers during 120 h. The obtained results revealed that the synthesized fibers are good candidates for loading of anticancer drugs.

References

- Abasian, P., Radmansouri, M., Jouybari, M. H., Ghasemi, M. V., Mohammadi, A., Irani, M., & Jazi, F. S. (2019). Incorporation of magnetic NaX zeolite/DOX into the PLA/chitosan nanofibers for sustained release of doxorubicin against carcinoma cells death in vitro. *International Journal of Biological Macromolecules*, 121(1), 398-406. <https://doi.org/10.1016/j.ijbiomac.2018.09.215>
- Aboutalebi Anaraki, N., Roshanfekar Rad, L., Irani, M., & Haririan, I. (2015). Fabrication of PLA/PEG/MWCNT electrospun nanofibrous scaffolds for anticancer drug delivery. *Journal of applied polymer science*, 132(3), 1-9. <https://doi.org/10.1002/app.41286>
- Alishiri, M., Shojaei, A., Abdekhodaie, M., & Yeganeh, H. (2014). Synthesis and characterization of biodegradable acrylated polyurethane based on poly (ϵ -caprolactone) and 1, 6-hexamethylene diisocyanate. *Materials Science and Engineering: C*, 42(1), 763-773. <https://doi.org/10.1016/j.msec.2014.05.056>
- Bahmani, E., Zonouzi, H. S., Koushkbaghi, S., Hafshejani, F. K., Chimeh, A. F., & Irani, M. (2020). Electrospun polyacrylonitrile/cellulose acetate/MIL-125/TiO₂ composite nanofibers as an efficient photocatalyst and anticancer drug delivery system. *Cellulose*, 27(17), 10029-10045. <https://doi.org/10.1007/s10570-020-03459-1>

- Bao, F., & Shi, W. (2010). Synthesis and properties of hyperbranched polyurethane acrylate used for UV curing coatings. *Progress in Organic Coatings*, 68(4), 334-339. <https://doi.org/10.1016/j.porgcoat.2010.03.002>
- Boissard, C., Bourban, P.-E., Tami, A., Alini, M., & Eglin, D. (2009). Nanohydroxyapatite/poly (ester urethane) scaffold for bone tissue engineering. *Acta Biomaterialia*, 5(9), 3316-3327. <https://doi.org/10.1016/j.actbio.2009.05.001>
- Chen, I.-W., & Wang, X.-H. (2000). Sintering dense nanocrystalline ceramics without final-stage grain growth. *Nature*, 404(6774), 168-171. <https://doi.org/10.1038/35004548>
- Chen, J.-P., & Chang, Y.-S. (2011). Preparation and characterization of composite nanofibers of polycaprolactone and nanohydroxyapatite for osteogenic differentiation of mesenchymal stem cells. *Colloids and Surfaces B: Biointerfaces*, 86(1), 169-175. <https://doi.org/10.1016/j.colsurfb.2011.03.038>
- Demir, D., Güreş, D., Tecim, T., Genç, R., & Bölgen, N. (2018). Magnetic nanoparticle-loaded electrospun poly (ϵ -caprolactone) nanofibers for drug delivery applications. *Applied Nanoscience*, 8(6), 1461-1469. <https://doi.org/10.1007/s13204-018-0830-9>
- Dizaji, B. F., Azerbaijan, M. H., Sheisi, N., Goleij, P., Mirmajidi, T., Chogan, F., . . . Sharafian, F. (2020). Synthesis of PLGA/chitosan/zeolites and PLGA/chitosan/metal organic frameworks nanofibers for targeted delivery of Paclitaxel toward prostate cancer cells death. *International Journal of Biological Macromolecules*, 164(1), 1461-1474. <https://doi.org/10.1016/j.ijbiomac.2020.07.228>
- Eskitoros-Togay, Ş. M., Bulbul, Y. E., Tort, S., Korkmaz, F. D., Acartürk, F., & Dilsiz, N. (2019). Fabrication of doxycycline-loaded electrospun PCL/PEO membranes for a potential drug delivery system. *International journal of pharmaceuticals*, 565(1), 83-94. <https://doi.org/10.1016/j.ijpharm.2019.04.073>
- Farboudi, A., Mahboobnia, K., Chogan, F., Karimi, M., Askari, A., Banihashem, S., . . . Irani, M. (2020a). UiO-66 metal organic framework nanoparticles loaded carboxymethyl chitosan/poly ethylene oxide/polyurethane core-shell nanofibers for controlled release of doxorubicin and folic acid. *International Journal of Biological Macromolecules*, 150(1), 178-188. <https://doi.org/10.1016/j.ijbiomac.2020.02.067>
- Farboudi, A., Nouri, A., Shirinzad, S., Sojoudi, P., Davaran, S., Akrami, M., & Irani, M. (2020b). Synthesis of magnetic gold coated poly (ϵ -caprolactonediol) based polyurethane/poly (N-isopropylacrylamide)-grafted-chitosan core-shell nanofibers for controlled release of paclitaxel and 5-FU. *International Journal of Biological Macromolecules*, 150(1), 1130-1140. <https://doi.org/10.1016/j.ijbiomac.2019.10.120>
- Ghafoor, B., Aleem, A., Ali, M. N., & Mir, M. (2018). Review of the fabrication techniques and applications of polymeric electrospun nanofibers for drug delivery systems. *Journal of Drug Delivery Science and Technology*, 48(1), 82-87. <https://doi.org/10.1016/j.jddst.2018.09.005>
- Guelcher, S. A. (2008). Biodegradable polyurethanes: synthesis and applications in regenerative medicine. *Tissue Engineering Part B: Reviews*, 14(1), 3-17. <https://doi.org/10.1089/teb.2007.0133>
- Guelcher, S. A., Gallagher, K. M., Didier, J. E., Klinedinst, D. B., Doctor, J. S., Goldstein, A. S., . . . Hollinger, J. O. (2005). Synthesis of biocompatible segmented polyurethanes from aliphatic diisocyanates and diurea diol chain extenders. *Acta Biomaterialia*, 1(4), 471-484. <https://doi.org/10.1016/j.actbio.2005.02.007>
- Guelcher, S., Srinivasan, A., Hafeman, A., Gallagher, K., Doctor, J., Khetan, S., . . . Hollinger, J. (2007). Synthesis, in vitro degradation, and mechanical properties of two-component poly (ester urethane) urea scaffolds: effects of water and polyol composition. *Tissue engineering*, 13(9), 2321-2333. <https://doi.org/10.1089/ten.2006.0395>
- He, Y., Zhou, M., Wu, B., Jiang, Z., & Nie, J. (2010). Synthesis and properties of novel polyurethane acrylate containing 3-(2-hydroxyethyl) isocyanurate segment. *Progress in Organic Coatings*, 67(3), 264-268. <https://doi.org/10.1016/j.porgcoat.2009.11.005>
- Hofmann, A., Ritz, U., Verrier, S., Eglin, D., Alini, M., Fuchs, S., . . . Rommens, P. M. (2008). The effect of human osteoblasts on proliferation and neo-vessel formation of human umbilical vein endothelial cells in a long-term 3D co-culture on polyurethane scaffolds. *Biomaterials*, 29(31), 4217-4226. <https://doi.org/10.1016/j.biomaterials.2008.07.024>
- Irani, M., Sadeghi, G. M. M., & Haririan, I. (2017). A novel biocompatible drug delivery system of chitosan/temozolomide

- nanoparticles loaded PCL-PU nanofibers for sustained delivery of temozolomide. *International Journal of Biological Macromolecules*, 97(1), 744-751. <https://doi.org/10.1016/j.ijbiomac.2017.01.073>
- Jouybari, M. H., Hosseini, S., Mahboobnia, K., Boloursaz, L. A., Moradi, M., & Irani, M. (2019). Simultaneous controlled release of 5-FU, DOX and PTX from chitosan/PLA/5-FU/g-C3N4-DOX/g-C3N4-PTX triaxial nanofibers for breast cancer treatment in vitro. *Colloids and Surfaces B: Biointerfaces*, 179(1), 495-504. <https://doi.org/10.1016/j.colsurfb.2019.04.026>
- Khodadadi, M., Alijani, S., Montazeri, M., Esmaeilzadeh, N., Sadeghi-Soureh, S., & Pilehvar-Soltanahmadi, Y. (2020). Recent advances in electrospun nanofiber-mediated drug delivery strategies for localized cancer chemotherapy. *Journal of Biomedical Materials Research Part A*, 108(7), 1444-1458. <https://doi.org/10.1002/jbm.a.36912>
- Krol, P. (2007). Synthesis methods, chemical structures and phase structures of linear polyurethanes. Properties and applications of linear polyurethanes in polyurethane elastomers, copolymers and ionomers. *Progress in materials science*, 52(6), 915-1015. <https://doi.org/10.1016/j.pmatsci.2006.11.001>
- Nunes, C., Simske, S., Sachdeva, R., & Wolford, L. (1997). Long-term ingrowth and apposition of porous hydroxylapatite implants. *Journal of Biomedical Materials Research: An Official Journal of The Society for Biomaterials and The Japanese Society for Biomaterials*, 36(4), 560-563. [https://doi.org/10.1002/\(SICI\)1097-4636\(19970915\)36:4<560::AID-JBM15>3.0.CO;2-E](https://doi.org/10.1002/(SICI)1097-4636(19970915)36:4<560::AID-JBM15>3.0.CO;2-E)
- Ouyang, X., Ko, S.-H., Castro, J., & Lee, L. J. (2015). A kinetics study of diacrylic-styrene crosslinking copolymerization. *Journal of Polymer Research*, 22(8), 148-154. <https://doi.org/10.1007/s10965-015-0793-4>
- Pereira, I. H., Ayres, E., Patrício, P. S., Góes, A. M., Gomide, V. S., Junior, E. P., & Oréfice, R. L. (2010). Photopolymerizable and injectable polyurethanes for biomedical applications: synthesis and biocompatibility. *Acta Biomaterialia*, 6(8), 3056-3066. <https://doi.org/10.1016/j.actbio.2010.02.036>
- Qavamnia, S. S., Rad, L. R., & Irani, M. (2020). Incorporation of Hydroxyapatite/Doxorubicin into the Chitosan/Polyvinyl Alcohol/Polyurethane Nanofibers for Controlled Release of Doxorubicin and Its Anticancer Property. *Fibers and Polymers*, 21(8), 1634-1642. <https://doi.org/10.1007/s12221-020-9809-8>
- Radmansouri, M., Bahmani, E., Sarikhani, E., Rahmani, K., Sharifianjazi, F., & Irani, M. (2018). Doxorubicin hydrochloride-Loaded electrospun chitosan/cobalt ferrite/titanium oxide nanofibers for hyperthermic tumor cell treatment and controlled drug release. *International Journal of Biological Macromolecules*, 116(1), 378-384. <https://doi.org/10.1016/j.ijbiomac.2018.04.161>
- Rajzer, I. (2014). Fabrication of bioactive polycaprolactone/hydroxyapatite scaffolds with final bilayer nano-/micro-fibrous structures for tissue engineering application. *Journal of Materials Science*, 49(16), 5799-5807. <https://doi.org/10.1007/s10853-014-8311-3>
- Rasouli, S., Montazeri, M., Mashayekhi, S., Sadeghi-Soureh, S., Dadashpour, M., Mousazadeh, H., . . . Pilehvar-Soltanahmadi, Y. (2020). Synergistic anticancer effects of electrospun nanofiber-mediated codelivery of Curcumin and Chrysin: Possible application in prevention of breast cancer local recurrence. *Journal of Drug Delivery Science and Technology*, 55(1), 101402. <https://doi.org/10.1016/j.jddst.2019.101402>
- Shackelford, J. F. (1999). *Bioceramics-current status and future trends*. Paper presented at the Materials Science Forum. <https://doi.org/10.4028/www.scientific.net/MSF.293.99>
- Suslu, A., Albayrak, A., Urkmez, A., Bayir, E., & Cocen, U. (2014). Effect of surfactant types on the biocompatibility of electrospun HAp/PHBV composite nanofibers. *Journal of Materials Science: Materials in Medicine*, 25(12), 2677-2689. [10.1007/s10856-014-5286-1](https://doi.org/10.1007/s10856-014-5286-1)
- Tawa, T., & Ito, S. (2006). The role of hard segments of aqueous polyurethane-urea dispersion in determining the colloidal characteristics and physical properties. *Polymer journal*, 38(7), 686-693. <https://doi.org/10.1295/polymj.PJ2005193>
- Tsai, S.-W., Yu, W.-X., Hwang, P.-A., Huang, S.-S., Lin, H.-M., Hsu, Y.-W., & Hsu, F.-Y. (2018). Fabrication and characterization of strontium-substituted hydroxyapatite-CaO-CaCO₃ nanofibers with a mesoporous structure as drug delivery carriers. *Pharmaceutics*, 10(4), 179-193 <https://doi.org/10.3390/pharmaceutics10040179>
- Wang, F., Hu, J., & Tu, W. (2008). Study on microstructure of UV-curable polyurethane acrylate films. *Progress in Organic*

- Coatings*, 62(3), 245-250. <https://doi.org/10.1016/j.porgcoat.2007.12.005>
- Wang, X., Hu, Y., Song, L., Xing, W., Lu, H., Lv, P., & Jie, G. (2010). Effect of antimony doped tin oxide on behaviors of waterborne polyurethane acrylate nanocomposite coatings. *Surface and Coatings Technology*, 205(7), 1864-1869. <https://doi.org/10.1016/j.surfcoat.2010.08.053>
- Webster, T. J., Siegel, R. W., & Bizios, R. (1999). Osteoblast adhesion on nanophase ceramics. *Biomaterials*, 20(13), 1221-1227. [https://doi.org/10.1016/S0142-9612\(99\)00020-4](https://doi.org/10.1016/S0142-9612(99)00020-4)
- Yao, C., Li, X., Neoh, K., Shi, Z., & Kang, E. (2008). Surface modification and antibacterial activity of electrospun polyurethane fibrous membranes with quaternary ammonium moieties. *Journal of Membrane Science*, 320(1-2), 259-267. <https://doi.org/10.1016/j.memsci.2008.04.012>
- Zheng, F., Wang, S., Shen, M., Zhu, M., & Shi, X. (2013a). Antitumor efficacy of doxorubicin-loaded electrospun nano-hydroxyapatite-poly (lactic-co-glycolic acid) composite nanofibers. *Polymer Chemistry*, 4(4), 933-941. <https://doi.org/10.1039/C2PY20779F>
- Zheng, F., Wang, S., Wen, S., Shen, M., Zhu, M., & Shi, X. (2013b). Characterization and antibacterial activity of amoxicillin-loaded electrospun nano-hydroxyapatite/poly (lactic-co-glycolic acid) composite nanofibers. *Biomaterials*, 34(4), 1402-1412. <https://doi.org/10.1016/j.biomaterials.2012.10.071>